Composite Fibers

DOI: 10.1002/anie.201310656

Bioinspired Green Composite Lotus Fibers**

Mengxi Wu, Hua Shuai, Qunfeng Cheng, and Lei Jiang*

Abstract: *Owing to the growing global environmental problems, demands for environmentally friendly, fully biodegradable sustainable composites have substantially increased across various industries. Inspired by the composite structure of cocoon silk, we fabricated a fully green composite fiber (GCF) that is based on the lotus fiber (LF) and a biodegradable polymer, namely poly(vinyl alcohol) (PVA). After the formation of cross-linkages between the LF and PVA, the mechanical properties of this bioinspired GCF had substantially improved. In particular, the specific mechanical properties are superior to those of cocoon silk and other natural fibers. These findings suggest that LFs may be used as reinforcement materials for the fabrication of bulk green materials for various industries, such as the textile, medical, automobile, and aerospace industries.*

Owing to the growing global environmental problems, the demands for environmentally friendly, fully biodegradable sustainable composites have substantially increased in various industries, including the textile, packaging, automobile, aerospace, and medical industries.[1] Aside from the traditional green composites that consist of nondegradable thermoplastic polymers,[2] such as polyethylene (PE),[3] polyesters,[4] or poly(methyl methacrylate) (PMMA),[5] and thermosetting polymers,[6] such as epoxy and polyurethane, fully biodegradable composites,[7] which are composed of natural fibers and biodegradable resins,[8] have received a lot of attention as they are sustainable materials that are based on renewable resources.[9]

"The lotus roots may break, but the fiber remains joined" is an old Chinese saying. Lotus fiber (LF) is a new kind of natural fiber and features, compared to other traditional natural fibers, significant advantages, including simple cultivation techniques, low costs, and abundant resources.[10] As the mechanical properties of pure LF are inadequate,[11] it remains a great challenge to apply LF for the construction of high-performance green composites. As a typical green composite fiber,[12] cocoon silk represents an ideal solution for the construction of high-performance composites that are based on LF. The fibroin fibers of cocoon silk are coated with a thin film of a sericin sheath, which acts like a matrix and allows for an efficient transfer of load stress to the fibroin fibers. A recent study revealed that compared to pure fibroin fibers, the mechanical properties of cocoon silk could be improved by 20%[13] with a sericin loading of only 20–26.6 wt%,[13,14] which is far lower than that of conventional carbon-fiber-reinforced composites.

Inspired by the of composite structure of cocoon silk, we fabricated a green composite fiber (GCF) that is based on LF and a biodegradable polymer, namely poly(vinyl alcohol) (PVA). Through the formation of cross-linkages between LF and PVA, the mechanical properties of this bioinspired GCF could be substantially improved and are thus comparable to those of natural fibers, such as jute, hemp, kenaf, and sisal fibers. In particular, the specific tensile strength of the bioinspired GCF is greater than that of cocoon silk, and its specific modulus is three larger higher than that of cocoon silk. The synthesis of this bioinspired GCF demonstrates that LF structures may be used as reinforcement materials for the fabrication of bulk green materials for applications in various areas, including the textile, medical, automobile, and aerospace industries.

The LF is easily drawn out from the lotus stem (Figure 1a). A cross section of the lotus stem reveals that the vessels and tracheids are of many different sizes (Figure 1b).[11] The lotus fibers are orderly assembled in the vessels and tracheids in the shape of a helix (Figure 1c).[15] The lotus fiber is spun out with a left-handed spiral structure (Figure 1d),[15b] and several individual lotus fibers are conglutinated into one bundle (Figure 1e).[11] The individual lotus fiber has an elliptical or slightly oval shape with a diameter in the range of 3.0–6.0 μm (Figure 1f); the average diameter was calculated to be approximately 5.0 μm (for details, see the Supporting Information, Figure S1). This self-assembled structure verifies the old Chinese saying that was mentioned above. The intrinsic features of the LF bundles are very different from those of other natural fibers, which can be transformed into continuous fibers by making use of an ancient technology, namely spinning.[16] Then, the bioinspired green composite fiber (GCF) was fabricated following the procedure that is described in Figure 2. The lotus stem is fixed on motor 1, which rotates anticlockwise, and the lotus fiber bundles are spun out by motor 3, which rotates clockwise. The PVA solution is simultaneously sprayed out from nozzle 2 into tiny droplets and deposited on the LF bundles. Then, the GCF is continuously collected on a stick 4 (Figure S2). The diameter of the GCF depends on the lotus stem; therefore,

[*] Dr. M. X. Wu,[+] H. Shuai,[+] Prof. Q. F. Cheng, Prof. L. Jiang
Key Laboratory of Bio-inspired Smart Interfacial Science and Technology of Ministry of Education
Beijing Key Laboratory of Bio-inspired Energy Materials and Devices
School of Chemistry and Environment, BeiHang University
Beijing 100191 (P.R. China)
E-mail: cheng@buaa.edu.cn

[†] These authors contributed equally to this work.

[**] This work was supported by the National Research Fund for Fundamental Key Projects (2010CB934700), the National Natural Science Foundation of China (21273017, 51103004), the Program for New Century Excellent Talents in University (NCET-12-0034), the Beijing Nova Program (Z121103002512020), the Beijing Science and Technology Program (Z121100001312004), the Key Research Program of the Chinese Academy of Sciences (KJZD-EW-M01), and the 111 Project (No. B14009).

Supporting information for this article is available on the WWW under http://dx.doi.org/10.1002/anie.201310656.

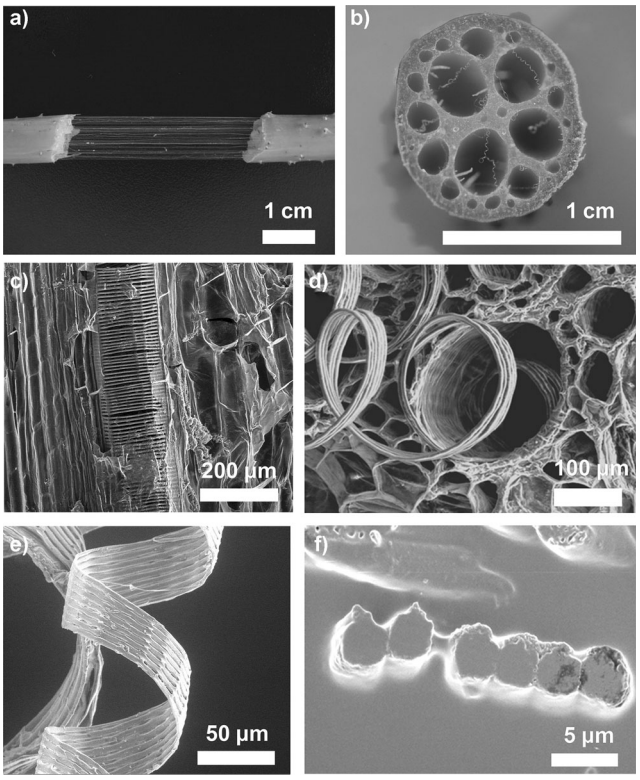

Figure 1. Morphology of natural lotus fibers. a) Digital image of lotus fibers drawn out from the stem. b) Spiral structure of lotus fibers that were assembled in the vessels and tracheids of a lotus stem. c) The SEM image reveals that the lotus fibers are orderly assembled in the vessels and tracheids in the shape of a helix. d) The lotus fibers can be spun out with a left-handed spiral structure. e) SEM image of one spiral lotus fiber bundle with conglutination of several lotus fibers. f) SEM image of the cross-section of one lotus fiber bundle.

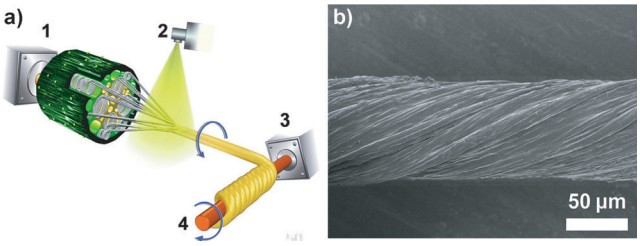

Figure 2. a) Setup for the fabrication of the bioinspired green composite fiber; for details, see the main text. b) A SEM image of GCF reveals a diameter of approximately 80.0 μm.

lotus stems with similar diameters were chosen for this study. The twist angle of the GCF is controlled by varying the ratio of the twisting speed and the collecting speed.[17]

During the spinning process, twisting is an effective approach for combining many single fibers into a high-performance fiber, especially for the fabrication of high-performance carbon nanotube fibers or yarn.[18] Herein, we fabricated five kinds of twisted LF fibers, including a single LF bundle, double, triple, and quadruple LF bundles, and whole LF bundles from one stem. The surface morphologies of these twisted LF bundles are shown in Figure S3 a–e.

The corresponding tensile stress–strain curves are shown in Figure S4 and the mechanical properties are shown in Table S1. The twisted single LF bundle displayed a tensile strength of 427.7 ± 17.5 MPa, a Young's modulus of 10.9 ± 1.7 GPa, and a toughness of 13.7 ± 7.1 MJ m^{-3}; these values are superior to those of materials that were previously prepared without twisting.[15a] However, for the twisted double LF bundles, the tensile strength decreased to 381.5 ± 50.3 MPa. When twisting more LF bundles, such as triple or quadruple LF bundles, the tensile strength substantially decreased to 211.1 ± 29.3 MPa and 174.6 ± 21.2 MPa, respectively. This is due to the fact that the twisted LF bundles are loose, and densification is very low, which can be clearly observed from the surface morphology of these twisted LF bundles and results in a poorly efficient load transfer. When all of the LF bundles were twisted into one fiber, the tensile strength can reach 329.4 ± 28.6 MPa, which is lower than the tensile strength of one twisted LF bundle, but still exceeds previously reported values.[15a] This is due to the fact that the densification of twisted LF bundles from the whole stem is higher than that of several twisted LF bundles, but lower that of one twisted LF bundle. The tensile stress–strain curves of twisted LF bundles also revealed similar phenomena (Figure S4). For the twisted single LF bundle, densification is very good, and the curve is sharply fractured. With increasing the number of twisted LF bundles, the tensile stress–strain curves show step failure with corresponding number of LF bundles (Figure S4 b–d). When whole LF bundles were twisted from one stem, the stress–strain curve showed the integration failure mode, indicating that the densification of twisted LF fibers had proceeded efficiently. Thus, we turned to fabricating the bioinspired GCF through twisting the whole LF bundles from one stem.

The twist angle is the key parameter of the twist process and is defined as the angle between the longitudinal direction of an individual fiber and the axis of the twisted fiber. Efficiently controlling the twist angle is helpful to obtain a twisted fiber with the desired mechanical properties. Several experiments and modeling studies have demonstrated that whereas the mechanical properties of a twisted fiber are improved by a small twist angle, they are worsened by a large twist angle.[18d] Herein, the LF bundles were twisted into fibers with three different twist angles: 10°, 15°, and 20° (for the corresponding SEM images, see Figure S5). The tensile strength of the twisted LF with an angle of 20° was found to be much higher than that of the twisted LFs with angles of 10° and 15°, which is consistent with previous reports on carbon nanotube fibers.[18b,c] Then, the twist angle of the bioinspired GCF was set to be approximately 20°. Inspired by cocoon silk,[13,14] the PVA matrix content was controlled to be in the range of 20.0–26.6 wt % by adjusting the concentration of the PVA solution. Three PVA solutions with different concentrations were used (1, 3, and 5 wt %), and the corresponding GCFs were designated as GCF-I, GCF-II, and GCF-III, respectively. The accurate PVA loadings of GCF-I, GCF-II, and GCF-III were calculated by thermogravimetric analysis (TGA) to be approximately 10.4, 22.4, and 37.3 wt %, respectively (Figure S6). The diameter of GCF-II is approximately 80.0 μm (Figure 2 b). The PVA loading of GCF-II

(22.4 wt%) is close to that of cocoon silk. The surface morphologies of GCF-I, GCF-II, and GCF-III were determined by SEM (Figure S7) and further confirmed the results from TGA. The PVA coating of GCF-1 is obviously not thick enough to hold the LF bundles tightly together, whereas the PVA coating of GCF-III is too thick. For GCF-II, however, the PVA coating has the appropriate thickness for holding the LF bundles together. The corresponding mechanical properties of these materials were also tested (Figure S8). The tensile strengths of GCF-I, GCF-II, and GCF-III were determined to be 439.5 ± 109.9 MPa, 622.5 ± 60.3 MPa, and 559.3 ± 54.8 MPa, respectively. Among these three GCFs, GCF-II displayed the best mechanical properties.

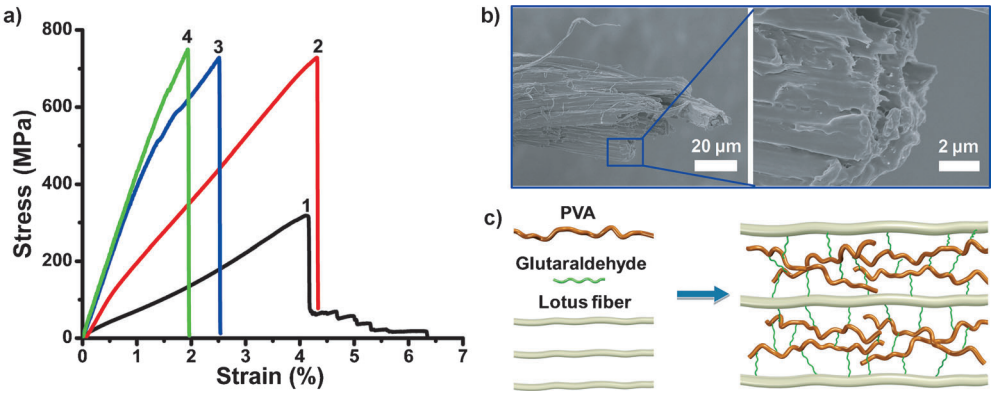

Figure 3. Mechanical properties of pure LF and bioinspired GCF-II before and after cross-linking. a) Stress–strain curves of pure LF (——), GCF-II (——), GCF-II with GA cross-linking (——), and GCF-II after both GA cross-linking and heat treatment (——). b) A SEM image of GCF-II after GA cross-linking and heat treatment reveals a typical brittle fracture morphology that is due to strong interfacial interactions between LF and PVA. c) Cross-linking of PVA and LF by GA. The formation of covalent acetal bridges between LF bundles and PVA substantially enhanced the interfacial strength.[22]

For composite materials, the interface plays a key role in determining the mechanical properties. Therefore, by improving the interface strength between LF and PVA, a substantial improvement of the mechanical properties of the bioinspired GCF should be possible. Based on the strategies that have been used for cross-linking PVA,[19] two approaches were applied to improve the interface strength between PVA and LF. One method entails the introduction of the highly efficient cross-linking agent glutaraldehyde (GA),[20] whereas the other approach is based on a heat treatment to cross-link the PVA matrix.[21] Before treating a GCF, a pure PVA film was subjected to both methods for an optimization of parameters. Tensile stress–strain curves of a pure PVA film and of PVA that had been subjected to different conditions are shown in Figure S9. The pure PVA film displayed a tensile strength of only 76.1 ± 4.2 MPa, a Young's modulus of 2.4 ± 0.3 GPa, and strain of 456.5 ± 87.9%. After cross-linking with GA, the tensile strength increased to 93.6 ± 14.9 MPa and 118.2 ± 35.3 MPa for PVA/GA ratios of 1:0.1 and 1:1, respectively. The heat treatment (60 °C for 2 h) enhanced the tensile strength up to 148.8 ± 7.3 MPa, which indicates that the cross-linking proceeded with high efficiency. When the heat treatment is combined with the method for GA cross-linking, the tensile strength of treated PVA can reach 202.7 ± 41.2 MPa, which is almost three times larger than that of pure PVA.

Therefore, two approaches, namely GA cross-linking and a combination of Ga cross-linking and the heat treatment were utilized to improve the mechanical properties of bioinspired GCF. The typical stress–strain curves of pure LF, GCF-II, GCF-II with GA cross-linking, and GCF-II after both GA cross-linking and the heat treatment are shown in Figure 3a. The tensile strength and Young's modulus of bioinspired GCF-II were determined to be 622.5 ± 60.3 MPa and 22.4 ± 2.9 GPa, respectively, and are thus larger than those of industrial *Bombyx mori* silk (tensile strength: 620.5 MPa; Young's modulus: 20.5 GPa).[13] After GA cross-linking, the tensile strength and the Young's modulus of bioinspired GCF-II had improved to 669.6 ± 82.9 MPa and 35.4 ± 8.9 GPa, respectively. When combining GA cross-linking and the heat treatment, the tensile strength and Young's modulus of bioinspired GCF-II were further enhanced to 714.3 ± 48.5 MPa and 43.4 ± 1.3 GPa, respectively. The maximum tensile strength reached 749 MPa, which is 20% larger than that of cocoon silk,[13] and comparable to that of other natural commercial fibers, such as flax, cotton, jute, hemp, sisal, and ramie fibers. The fracture morphology of GCF-II after both GA cross-linking and the heat treatment revealed a typical brittle fracture feature, and no delamination occurred between the LF bundles and PVA (Figure 3b), indicating strong interfacial interactions between the LF bundles and PVA after treatment by combining GA and heat. The proposed mechanism for cross-linking after GA treatment is shown in Figure 3c. The formation of covalent acetal bridges between the LF bundles and PVA[22] was confirmed by FTIR spectroscopy (Figure S10). The characteristic peaks of secondary alcohols at approximately 1100 cm^{-1} that were observed for LF bundles and PVA disappeared after GA treatment.

The mechanical properties of bioinspired GCF and other natural fibers are listed in Table S2. The density of the lotus fiber is only 1.18 $g\,cm^{-3}$,[23] which is lower than that of other natural fibers. Thus, when their densities are taken into account, the specific mechanical properties of bioinspired GCF are better than those of commercial fibers. The specific tensile strength of the bioinspired GCF reached 629 $kN\,m^{-1}\,kg^{-1}$, which is higher than that of cocoon silk[24] and other natural fibers, including cotton, jute, hemp, sisal, ramie fibers,[7a] and comparable to that of flax fiber ($\leq$690 $kN\,m^{-1}\,kg^{-1}$; Figure 4).[1] The specific modulus of bioinspired GCF was measured to be as high as 37.8 $MN\,m^{-1}\,kg^{-1}$, which is three times larger than that of

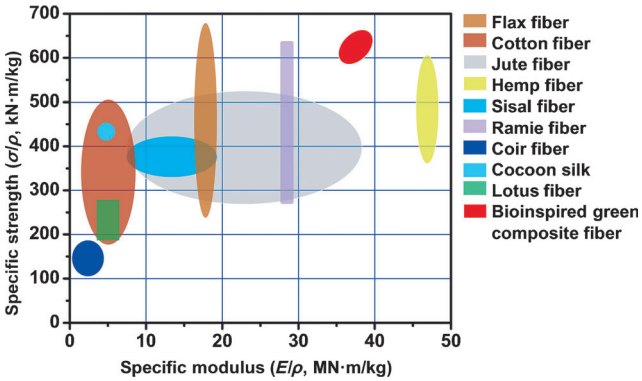

Figure 4. Comparison of specific mechanical properties of the bioinspired green composite fiber with those of commercial natural fibers, such as flax, cotton, jute, hemp, sisal, ramie, and coir fibers, and cocoon silk.

cocoon silk (10.4 MN m^{-1} kg^{-1}),[24] close to that of hemp fiber (47 MN m^{-1} kg^{-1}),[7a] and larger than that of other natural fibers.[7a] The efficient cross-linking between LF and PVA in the bioinspired GCF further improved the load transfer from the matrix to the lotus fiber, which results in outstanding mechanical properties.

In conclusion, inspired by the composite structure of cocoon silk, we fabricated a green composite fiber (GCF) based on a novel green lotus fiber. The specific tensile strength of GCF is comparable to that of flax fiber and larger than that of other commercial natural fibers and cocoon silk. The specific modulus of GCF is three times higher than that of cocoon silk. This novel bioinspired strategy represents an efficient approach for improving the mechanical properties of natural fibers and opens the door towards the biomimetic production of natural composite fibers with superior mechanical properties for applications in diverse industries, including the medical, automobile, and aerospace industries.

Experimental Section

Materials: Lotus stems were collected near Tsinghua University, China. Poly(vinyl alcohol) (PVA; $M_w \approx 7500$) and glutaraldehyde (GA) were purchased from Sigma–Aldrich and used as received.

The fabrication process for bioinspired green composite fibers is described in Figure 2a. The two efficient approaches for cross-linking are based on the addition of glutaraldehyde and on a heat treatment.

Characterization: Mechanical tests were carried out on a Shimadzu AGS-X instrument with a loading rate of 1 mm min^{-1} and a gauge length of 5 mm. Scanning electron microscope images were obtained with a HITACHI S-4800 microscope. The thermal stability of the samples was determined by thermogravimetric analysis (TG/DTA6300, NSK). FTIR spectra were collected using a Thermo Nicolet nexus-470 FTIR spectrometer.

Received: December 9, 2013
Published online: February 7, 2014

Keywords: bioinspired chemistry · composite fibers · lotus fiber · mechanical properties · polymers

[1] A. N. Netravali, S. Chabba, *Mater. Today* **2003**, *6*, 22–29.
[2] S. J. Eichhorn, C. A. Baillie, N. Zafeiropoulos, L. Y. Mwaikambo, M. P. Ansell, A. Dufresne, K. M. Entwistle, P. J. Herrera-Franco, G. C. Escamilla, L. Groom, M. Hughes, C. Hill, T. G. Rials, P. M. Wild, *J. Mater. Sci.* **2001**, *36*, 2107–2131.
[3] K. Joseph, S. Thomas, C. Pavithran, M. Brahmakumar, *J. Appl. Polym. Sci.* **1993**, *47*, 1731–1739.
[4] a) P. Zadorecki, H. Karnerfors, S. Lindenfors, *Compos. Sci. Technol.* **1986**, *27*, 291–303; b) L. Hua, P. Flodin, T. Rönnhult, *Polym. Compos.* **1987**, *8*, 203–207.
[5] G. Canché-Escamilla, J. Rodriguez-Laviada, J. I. Cauich-Cupul, E. Mendizábal, J. E. Puig, P. J. Herrera-Franco, *Composites Part A* **2002**, *33*, 539–549.
[6] D. N. Saheb, J. P. Jog, *Adv. Polym. Technol.* **1999**, *18*, 351–363.
[7] a) H.-y. Cheung, M.-p. Ho, K.-t. Lau, F. Cardona, D. Hui, *Composites Part B* **2009**, *40*, 655–663; b) E. Zini, M. Scandola, *Polym. Compos.* **2011**, *32*, 1905–1915; c) M. J. John, S. Thomas, *Carbohydr. Polym.* **2008**, *71*, 343–364.
[8] A. K. Mohanty, M. Misra, G. Hinrichsen, *Macromol. Mater. Eng.* **2000**, *276–277*, 1–24.
[9] O. Faruk, A. K. Bledzki, H.-P. Fink, M. Sain, *Prog. Polym. Sci.* **2012**, *37*, 1552–1596.
[10] K. M. M. Rao, K. M. Rao, *Compos. Struct.* **2007**, *77*, 288–295.
[11] D. Liu, G. T. Han, J. C. Huang, Y. M. Zhang, *Carbohydr. Polym.* **2009**, *75*, 39–43.
[12] Z. Z. Shao, F. Vollrath, *Nature* **2002**, *418*, 741.
[13] V. Jauzein, A. Bunsell, *J. Mater. Sci.* **2012**, *47*, 3082–3088.
[14] a) P. Jiang, H. Liu, C. Wang, L. Wu, J. Huang, C. Guo, *Mater. Lett.* **2006**, *60*, 919–925; b) C. S. Ki, J. W. Kim, H. J. Oh, K. H. Lee, Y. H. Park, *Int. J. Biol. Macromol.* **2007**, *41*, 346–353.
[15] a) Y. Pan, G. T. Han, Z. P. Mao, Y. M. Zhang, H. Duan, J. C. Huang, L. J. Qu, *Carbohydr. Polym.* **2011**, *85*, 188–195; b) K. Kamata, S. Suzuki, M. Ohtsuka, M. Nakagawa, T. Iyoda, A. Yamada, *Adv. Mater.* **2011**, *23*, 5509–5513.
[16] E. J. W. Barber, *Prehistoric Textiles*, Princeton Univ. Press, Princeton, **1992**.
[17] K. Liu, Y. H. Sun, X. Y. Lin, R. F. Zhou, J. P. Wang, S. S. Fan, K. L. Jiang, *ACS Nano* **2010**, *4*, 5827–5834.
[18] a) K. Liu, Y. H. Sun, R. F. Zhou, H. Y. Zhu, J. P. Wang, L. Liu, S. S. Fan, K. L. Jiang, *Nanotechnology* **2010**, *21*, 045708; b) W. J. Ma, L. Q. Liu, R. Yang, T. H. Zhang, Z. Zhang, L. Song, Y. Ren, J. Shen, Z. Q. Niu, W. Y. Zhou, S. S. Xie, *Adv. Mater.* **2009**, *21*, 603–608; c) X. Zhang, Q. Li, Y. Tu, Y. Li, J. Y. Coulter, L. Zheng, Y. Zhao, Q. Jia, D. E. Peterson, Y. Zhu, *Small* **2007**, *3*, 244–248; d) Y. Rao, R. J. Farris, *J. Appl. Polym. Sci.* **2000**, *77*, 1938–1949; e) M. Zhang, K. R. Atkinson, R. H. Baughman, *Science* **2004**, *306*, 1358–1361.
[19] B. Bolto, T. Tran, M. Hoang, Z. Xie, *Prog. Polym. Sci.* **2009**, *34*, 969–981.
[20] a) M. Nagy, E. Wolfram, T. Varadi, *Prog. Colloid Polym. Sci.* **1976**, *60*, 138–146; b) D. Braun, E. Walter, *Colloid Polym. Sci.* **1980**, *258*, 795–801.
[21] a) M. G. Katz, T. Wydeven, *J. Appl. Polym. Sci.* **1982**, *27*, 79–87; b) A. Amanda, S. K. Mallapragada, *Biotechnol. Prog.* **2001**, *17*, 917–923.
[22] P. Podsiadlo, A. K. Kaushik, E. M. Arruda, A. M. Waas, B. S. Shim, J. Xu, H. Nandivada, B. G. Pumplin, J. Lahann, A. Ramamoorthy, N. A. Kotov, *Science* **2007**, *318*, 80–83.
[23] J. Wang, X. Yuan, J. He, Y. Gan, D. Chen, *J. Text. Res.* **2008**, *29*, 9–11.
[24] J. M. Gosline, P. A. Guerette, C. S. Ortlepp, K. N. Savage, *J. Exp. Biol.* **1999**, *202*, 3295–3303.
[25] A. K. Bledzki, S. Reihmane, J. Gassan, *J. Appl. Polym. Sci.* **1996**, *59*, 1329–1336.